Biochemical Journal (2016) **473** 4243–4254
DOI: 10.1042/BCJ20160674

PORTLAND PRESS

Research Article

Regulation of divalent metal transporter-1 by serine phosphorylation

Young Ah Seo*, Ruvin Kumara*, Herbert Wetli and Marianne Wessling-Resnick

Department of Genetics and Complex Diseases, Harvard School of Public Health, Boston, MA, USA

Correspondence: Marianne Wessling-Resnick (wessling@hsph.harvard.edu)

OPEN ACCESS

Divalent metal transporter-1 (DMT1) mediates dietary iron uptake across the intestinal mucosa and facilitates peripheral delivery of iron released by transferrin in the endosome. Here, we report that classical cannabinoids (Δ^9-tetrahydrocannabinol, Δ^9-THC), nonclassical cannabinoids (CP 55,940), aminoalkylindoles (WIN 55,212-2) and endocannabinoids (anandamide) reduce ^{55}Fe and ^{54}Mn uptake by HEK293T(DMT1) cells stably expressing the transporter. siRNA knockdown of cannabinoid receptor type 2 (CB2) abrogated inhibition. CB2 is a G-protein (GTP-binding protein)-coupled receptor that negatively regulates signal transduction cascades involving serine/threonine kinases. Immunoprecipitation experiments showed that DMT1 is serine-phosphorylated under basal conditions, but that treatment with Δ^9-THC reduced phosphorylation. Site-directed mutation of predicted DMT1 phosphosites further showed that substitution of serine with alanine at N-terminal position 43 ($S^{43}A$) abolished basal phosphorylation. Concordantly, both the rate and extent of ^{55}Fe uptake in cells expressing DMT1($S^{43}A$) was reduced compared with those expressing wild-type DMT1. Among kinase inhibitors that affected DMT1-mediated iron uptake, staurosporine also reduced DMT1 phosphorylation confirming a role for serine phosphorylation in iron transport regulation. These combined data indicate that phosphorylation at serine 43 of DMT1 promotes transport activity, whereas dephosphorylation is associated with loss of iron uptake. Since anti-inflammatory actions mediated through CB2 would be associated with reduced DMT1 phosphorylation, we postulate that this pathway provides a means to reduce oxidative stress by limiting iron uptake.

Introduction

Divalent Metal Transporter-1 (DMT1; Slc11A2) mediates ferrous (Fe^{2+}) iron uptake across the small intestine [1] and the delivery of iron to peripheral tissues by transferrin [2]. Electrophysiological studies have shown that DMT1 not only transports Fe^{2+}, but that it also interacts with other divalent metals [3]. DMT1 activity is voltage and pH-dependent [4]. The *SLC11A2* gene encoding DMT1 produces multiple isoforms through alternative promoters (1A or 1B) and/or alternative splicing to produce transcripts with or without an iron regulatory element (+IRE or −IRE) [5]. While 1A isoforms are predominantly expressed in duodenum and kidney, 1B isoforms are ubiquitously expressed [5]. The 1A isoform is regulated by hypoxia-inducible factor 2α response elements that increase intestinal DMT1 expression in response to hypoxia [6,7]. Protein levels of the +IRE isoforms increase during times of deficiency, and iron-dependent post-transcriptional control of IRE-containing DMT1 transcripts by iron regulatory proteins has been demonstrated [8,9]. The membrane proteins generated by various DMT1 transcripts have different subcellular targeting. All DMT1 isoforms display similar function and equal efficiency, but the 1A/+IRE isoform is predominantly detected at the plasma membrane, whereas the 1A/−IRE, 1B/+IRE and 1B/−IRE isoforms are more abundant in intracellular compartments [10,11]. The tissue-specific expression and subcellular localization of different DMT1 isoforms may regulate iron transport by distinct membranes and organelles in different cell types. In addition, DMT1 is regulated post-translationally by ubiquitination mediated through Ndfips (NEDD4 family-interacting

*Both authors contributed equally to this work.

Received: 14 July 2016
Revised: 22 September 2016
Accepted: 28 September 2016

Accepted Manuscript online: 28 September 2016
Version of Record published: 10 November 2016

PORTLAND PRESS

Biochemical Journal (2016) 473 4243–4254
DOI: 10.1042/BCJ20160674

protein 2) and WWP2 (WW domain-containing E3 ubiquitin protein ligase 2), which control its degradation [12]. In summary, DMT1 expression and activity are highly regulated at the transcriptional, post-transcriptional and post-translational levels. Since excess iron is associated with oxidative stress and cytotoxicity, these various mechanisms controlling iron assimilation by DMT1 are critical to maintaining cellular homeostasis.

Small molecule inhibitors can help to further identify factors involved in the regulation of iron transport activity. Our previous screen of bioactive molecules revealed that the cannabinoid Δ^9-tetrahydrocannabinol (Δ^9-THC) inhibits DMT1 function [13]. Δ^9-THC effects are mediated through cannabinoid receptors (cannabinoid receptor type 1, CB1 and cannabinoid receptor type 2, CB2), members of the G-protein (GTP-binding protein)-coupled receptor class [14]. The cannabinoid system has been implicated in many physiological functions, both in the central and peripheral nervous system and in peripheral organs, providing a therapeutic target for many pathological conditions [15]. In particular, the cannabinoid system has been shown to negatively couple to N- and P/Q-type voltage-operated Ca^{2+} channels [16–18] and positively couple to A-type and inwardly rectifying K^+ channels [19,20]. Cannabinoids have also been shown to inhibit acid-sensing channels [21] and Na^+-dependent amino acid transporters [22]. We undertook this study to determine the mechanism through which Δ^9-THC inhibits DMT1-mediated iron transport, since this pathway would also provide therapeutic opportunities to limit assimilation to prevent iron overload diseases.

Experimental procedures

Plasmid construction

The hemagglutinin (HA)-tagged mouse DMT1 (non-IRE exon 1B isoform) plasmid [23] was generously provided by Dr Philippe Gros (McGill University). In this construct, the HA tag (YPYDVPDYA) is inserted in the predicted extracellular domain between transmembrane domains 7 and 8 [24]. Previous work by this group has characterized the transport activity [24,25] and membrane trafficking [26,27] of this construct to demonstrate its compatibility with properties of wild-type DMT1 (non-IRE 1B). In the present study, site-directed mutations on this plasmid (S^{21}A-HA, S^{23}A-HA, S^{32}A-HA, S^{39}A-HA and S^{43}A-HA) were constructed using the QuikChange® II XL kit (Stratagene, La Jolla, CA, USA) according to the manufacturer's protocol. The site-directed mutation, orientation and fidelity of the inserts, and incorporation of the epitope tags, were confirmed by directed sequencing (Dana Farber/Harvard Cancer Center DNA Resource Core).

Cell culture and transient transfection

HEK293T(DMT1) cells [13] were cultured in α-minimal essential medium supplemented with 50 U/ml penicillin, 50 μg/ml streptomycin and 10% fetal bovine serum. To transiently express HA-tagged DMT1 (DMT1-HA), parental HEK293T cells were transfected with 0.5 μg (24-well plates), 4 μg (6-well plates) or 24 μg (10 cm^2 dishes) of wild-type or mutant alleles of DMT1 plasmid in serum- and antibiotic-free medium using Lipofectamine 2000 (Invitrogen) at a DNA:transfection reagent ratio of 1:2.5 according to the manufacturer's specifications. Transfection medium was replaced 4–6 h later with antibiotic-free growth medium, and cells were cultured for an additional 24 h prior to experiments.

Transport studies with radioisotopic tracer

HEK293T(DMT1) cells were grown to 60–80% confluence in 10-cm plates, and washed three times with PBS containing 1 mM $MgCl_2$ and 0.1 mM $CaCl_2$ (PBS++), and lifted by carefully pipetting up and down into PBS++ or uptake buffer (25 mM Tris, 25 mM MES, 140 mM NaCl, 5.4 mM KCl, 1.8 mM $CaCl_2$, 0.8 mM $MgSO_4$ and 5 mM glucose, pH 6.75). Cell counts were determined and samples were aliquoted for studies. Δ^9-THC (Sigma), CP 55,940 (Tocris Bioscience), WIN 55,212-2 (Tocris Bioscience), anandamide (Tocris Bioscience), staurosporine (LC Laboratories), H-7, GDPβS, Sp-8-bromo-cAMP (Sigma Chemical Co.), U0126-EtOH, trametinib or PD0325902 (Selleck Chemicals) were added to cell aliquots at the indicated concentrations and compared with control cell aliquots treated with the appropriate vehicle (water or 0.5% DMSO, v/v). In the standard assay, cells were incubated at 37°C for 20 min in uptake buffer containing 1 μM ^{55}Fe and 50 μM ascorbic acid (pH 6.75). Cells were chilled on ice, collected on nitrocellulose filters and washed three times by centrifugation or vacuum filtration with ice-cold PBS to remove any unbound ^{55}Fe or ^{54}Mn. Cells were lysed with solubilization buffer (0.1% Triton X-100/0.1% NaOH), and cell-associated radioactivity was determined by scintillation counting. Uptake was calculated as pmol per million cells per min and was normalized to control (vehicle alone) to determine the extent of inhibition in the presence of a drug as indicated in the legends. In

Biochemical Journal (2016) **473** 4243–4254
DOI: 10.1042/BCJ20160674

experiments employing HEK293T cells transiently expressing DMT1 and various mutants, transport assays were carried out for the times indicated in the figures and legends by using individual wells that were each separately transfected. In these experiments, cells from each well were lysed and uptake was measured by scintillation counting, then adjusted to lysate cell protein for that individual well measured using the Bradford assay. Uptake is shown as pmol/mg protein.

Small interfering RNA-mediated gene suppression of cannabinoid receptor

HEK293T(DMT1) cells (1×10^5 cells per well) were plated in six-well plates overnight and then transfected with 100 nM of control siRNA (Ambion), CB1 siRNA (CNR1-s3261, Ambion) or CB2 siRNA (CNR2-s3263, Ambion) using Lipofectamine 2000 (Invitrogen) as described above. After 24 h incubation, the transfection medium was replaced with serum-containing, antibiotic-free medium, and cells were cultured for another 16 h before experiments. Cells were collected for the determination of CB1 and CB2 protein abundance and ^{55}Fe uptake.

Immunoblot analysis

Cells were washed twice with ice-cold PBS, and the total cell lysates were prepared in lysis buffer containing 150 mM NaCl, 1 mM EDTA, 50 mM Tris and 1% Triton containing a protease inhibitor cocktail (Complete Mini, Roche). Protein concentration was determined by the Bradford assay. Samples (25 μg) were separated by electrophoresis on 10% SDS–PAGE gels and transferred to PVDF membranes, and immunoblotted with rabbit anti-CB1 or -CB2 antibody (Cayman Chemical Company). The primary antibody was detected with IRDye 800-conjugated secondary antibodies (Rockland Immunochemicals, Inc.). After further washing, immunoreactivity was detected by an Odyssey Infrared Imaging System (Li-COR).

Immunoprecipitation experiments

To determine HA-DMT1 phosphorylation, cells transfected with HA-DMT1 or empty vector were scraped into ice-cold PBS and pelleted by centrifugation, then lysed in Nonidet-P40 (NP-40) buffer (40 mM HEPES, pH 7.4, 120 mM NaCl, 5% glycerol, 1% NP-40 and 1 mM EDTA, pH 8.0) containing phosphatase inhibitors (10 mM pyrophosphate, 10 mM β-glycerophosphate, 50 mM NaF and 0.5 mM orthovanadate) for 30 min at 4°C with rotation. Samples were centrifuged for 10 min at 15 000×***g***, and the protein concentration of the lysates was determined by the Bradford assay. The cell lysates were preincubated with anti-HA agarose (Pierce) overnight at 4°C with rotation and washed with TBS before protein elution at 95°C for 5 min. Eluates were electrophoresed on 4–20% gradient gels, transferred to PVDF membranes and the extent of HA-DMT1 phosphorylation was assessed by immunoblotting with mouse antiphosphoserine antibody (Millipore) followed by IRDye 800-conjugated secondary antibodies (Rockland Immunochemicals). Meanwhile, total cell lysates were immunoblotted with either anti-HA antibody or by antiactin antibody followed by IRDye800-conjugated secondary antibodies. After further washing, immunoreactivity was detected by an Odyssey Infrared Imaging System (Li-COR).

Statistical analysis

Statistical comparisons were determined using unpaired Student's *t*-test (Prism Graph Pad, Berkeley, CA, USA). In Figure 1, dose–response curves were best fit by a Hill four-parameter sigmoidal model with analysis made using Sigmaplot (Systat software). In Figure 2B, data were analyzed by two-way ANOVA followed by Holm–Sidak's multiple comparisons test for pairwise comparisons. In Figure 4C, where comparisons were made by one-way ANOVA followed by Tukey post hoc analysis. Results shown are means ± SEM unless otherwise indicated. For all statistical analyses, results were considered significant at $P < 0.05$.

Results

Cannabinoids inhibit DMT1-mediated iron (II) uptake

Our previous study showed that Δ^9-THC inhibited DMT1 activity with an IC_{50} of ∼0.45 μM [13]. We further examined the effect of different types of cannabinoids on iron uptake using an ^{55}Fe tracer assay. Inhibition of HEK293T cells stably overexpressing DMT1 by the endogenous cannabinoid anandamide, and synthetic cannabinoids structurally unrelated to the 'classic cannabinoid Δ^9-THC, including the so-called nonclassical cannabinoid CP 55,940 and the aminoalkylindole agonist WIN 55,212-2, was examined (Figure 1A). The IC_{50} values were all below 10 μM (see table in Figure 1). The values for *y*(min) determined from regression analysis suggest an index of efficacy of CP 55,940 (30.9%) > anandamide (36.1%) > WIN 55,121-2 (56.8%). These

Biochemical Journal (2016) 473 4243–4254
DOI: 10.1042/BCJ20160674

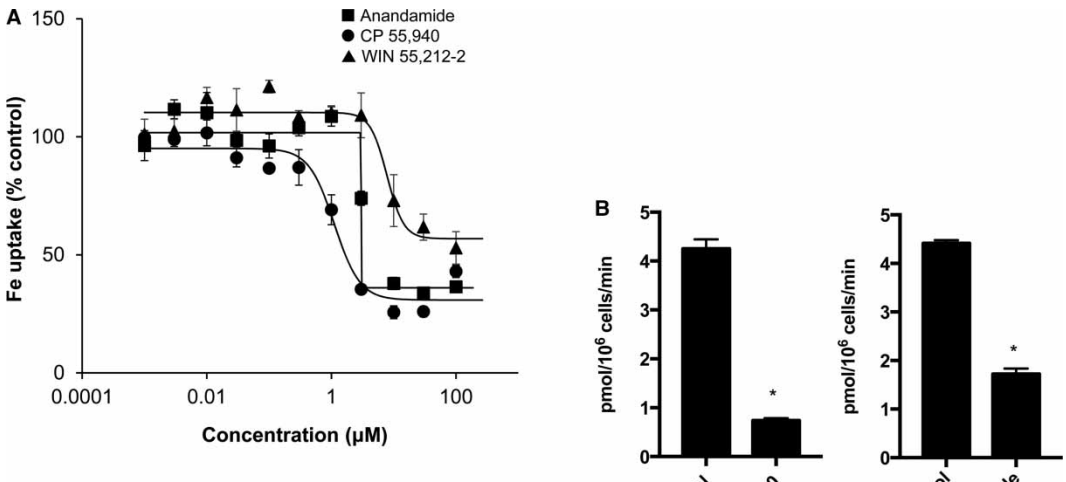

Parameter	Anandamide	CP 55,940	WIN 55,212-2
Ymax (%)	103.5	92.22	113.9
Ymin (%)	36.1	31.3	56.0
P value	<0.0001	0.0009	0.0002
R^2	0.9817	0.9550	0.9742
IC_{50} (μM)	3.03	1.18	7.19

Figure 1. Dose–response studies of DMT1 inhibition by cannabinoids.

HEK293T(DMT1) cells were incubated at 37°C for 20 min with 0.001–100 μM of the indicated compounds as described in the Experimental Procedures section ($n = 6$). Shown are curves fit by regression analysis with symbols indicated in (**A**). (**B**) ^{54}Mn uptake in the absence and presence of 50 μM anandamide or CP55,940. Shown are means (±SEM) for control cells incubated with vehicle (DMSO) and indicated drug ($n = 3$); results from one experiment with similar results obtained on at least one other occasion (*$P < 0.0001$). Dose response curves were best fit by a Hill four-parameter sigmoidal model with values obtained for Ymax, Ymin, and IC_{50} shown in the inserted table. The P-values and R^2 for each of the curve fits are also provided.

combined data indicate that both exogenous and endogenous cannabinoids inhibit DMT1-mediated iron uptake in a dose-dependent manner. Since DMT1 transports other divalent metals, we also confirmed the effects of cannabinoids on ^{54}Mn uptake, which was reduced by anandamide and CP 55,940 (Figure 1B).

CB2 mediates inhibition by Δ^9-THC

Cannabinoids produce many biological effects primarily mediated through interactions with cannabinoid receptors CB1 and CB2 [14]. To determine whether iron transport inhibition by Δ^9-THC was due to interactions of either cannabinoid receptor, we used siRNA to knockdown CB1 and CB2 in HEK293T(DMT1) cells. Western blot analysis showed that CB1 and CB2 receptors were effectively reduced compared with control cells (Figure 2A). DMT1-mediated ^{55}Fe uptake and its response to Δ^9-THC were unaffected by CB1 knockdown (Figure 2B). Knockdown of CB2 reduced the total amount of iron taken up in the absence of Δ^9-THC, at 2 μM Δ^9-THC and at 10 μM Δ^9-THC in CB2 siRNA-treated cells compared with the control siRNA-treated cells (Figure 2B). These results indicate that inhibition of iron transport is dependent on the expression of CB2. Under basal conditions, the presence of this receptor appears to enhance DMT1 activity, supporting the idea that cannabinoid agonists act through CB2 to suppress transporter function.

CB2 is a member of the G-protein-coupled receptor family and is known to negatively regulate adenylate cyclase through its interactions with Gi/Go α subunits. To further delineate its potential role in the regulation of DMT1-mediated iron transport, we studied activators and inhibitors of this signaling pathway (Figure 3). The treatment of HEK293T(DMT1) cells with the GDP analog GDPβS reduced iron uptake. In contrast, the Gi/o protein activator pertussis toxin enhanced transport. Likewise the cAMP agonist sp-8-Br-cAMP enhanced iron transport, consistent with the idea that negative regulation of adenylate cyclase leads to inhibition of DMT1 activity. H7, a cAMP-protein kinase (PKA) inhibitor, reduced iron transport by a small but reproducible

Biochemical Journal (2016) **473** 4243–4254
DOI: 10.1042/BCJ20160674

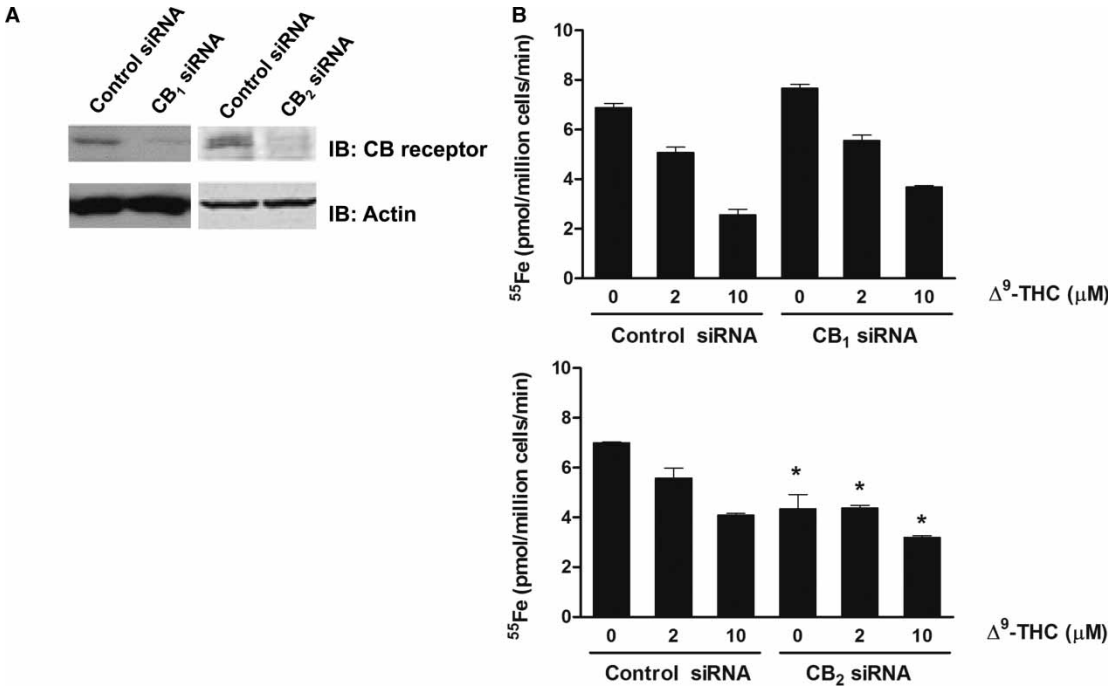

Figure 2. Loss of CB2 receptor abrogates Δ^9-THC inhibition of iron transport.

(**A**) A representative immunoblot of CB1 or CB2 receptor levels in cells transfected with control, CB1 or CB2 receptor-specific siRNA. Equal loading was verified by immunoblotting with antiactin antibody. (**B**) Inhibition of iron uptake by CB1 or CB2 receptor-attenuated cells incubated with 2 or 10 μM of Δ^9-THC. Results shown are means ± SEM from at least two independent experiments ($n = 5$). *Two-way ANOVA followed by Holm–Sidak's multiple comparisons test showed that CB2 knockdown reduced iron transport in the absence of Δ^9-THC ($P = 0.0003$), at 2 μM Δ9-THC ($P = 0.0114$) and at 10 μM Δ9-THC ($P = 0.0216$) compared with controls.

extent. Staurosporine, a broad spectrum PKA and protein kinase C (PKC) inhibitor, had a greater dose-dependent effect (see below). Through interactions with the G-protein βγ subunit, CB2 can also couple to mitogen-activated protein kinase/extracellular signal-regulated kinases (MAPK/ERK). We, therefore, also tested transport inhibition by the kinase inhibitors U0126-EtOH (50 μM), trametinib (5 μM) or PD0325902 (50 μM), but did not observe any significant or reproducible effects (data not shown).

Serine phosphorylation of DMT1 is blocked by Δ^9-THC

As discussed above, CB2 receptor signal transduction mechanisms regulate serine/threonine phosphorylation by many different kinases. To more directly examine possible phosphorylation of DMT1 and effects of Δ^9-THC, HEK293T cells were transfected to transiently express HA-tagged DMT1. These cells and control cells (transfected with empty plasmid) were treated with or without Δ^9-THC. Anti-HA antibodies were used to immunoprecipitate HA-DMT1 from cell lysates, which was then immunoblotted to detect phosphoserine. Antiphosphoserine antibodies were detected phosphorylation of HA-DMT1 in the absence of Δ^9-THC. The extent of DMT1 serine phosphorylation was reduced in cells treated with the cannabinoid (Figure 4A). The results are consistent with the idea that under basal conditions, active DMT1 is serine-phosphorylated and in response to CB2 activation, the inactivated transporter is dephosphorylated.

Two independent computer-assisted approaches that predict phosphorylation sites were used to examine potential DMT1 target residues: PhosphoSitePlus [28] and NetPhos 2.0 server [29]. Both algorithms revealed possible phosphosites in the N-terminal cytoplasmic domain (S^{21}, S^{23}, S^{32}, S^{39} and S^{43}) on DMT1 (Figure 4A). These residues are all conserved in four known protein isoforms of DMT1. To determine if these serine residues play a role in DMT1 phosphorylation, we replaced each serine residue individually with alanine by site-directed mutagenesis and tested HA-DMT1 phosphorylation. Our results showed that point mutation of serine to alanine at 43 ($S^{43}A$) completely abolished basal phosphorylation of DMT1 (Figure 4B).

Biochemical Journal (2016) 473 4243–4254
DOI: 10.1042/BCJ20160674

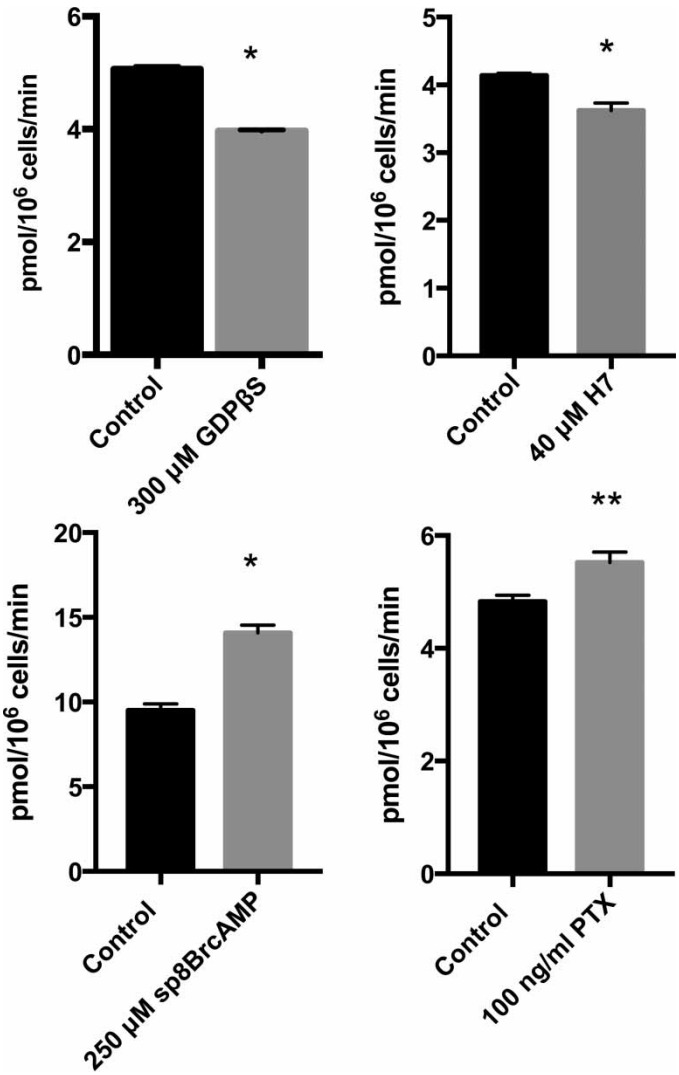

Figure 3. Inhibitors and activators of DMT1-mediated iron uptake.

Results of transport assays performed as described in Figure 1 are shown for indicated agents compared with vehicle control (0.5% DMSO, v/v, bottom panel) or water alone (top panel). Results are from single independent experiments' means ± SEM determined for biological triplicates with similar results obtained on at least two separate occasions. For pertussis toxin (PTX) experiments, cells were treated with 100 ng/ml toxin added to culture medium for at least 24 h prior to assays (*$P < 0.01$; **$P < 0.05$).

DMT1 phosphorylation at serine 43 promotes iron uptake

To confirm that S^{43} is a phosphorylation site important for DMT1 function, cells were transfected to express S^{43}A-HA. Control immunoprecipitation experiments confirmed that this mutant failed to be phosphorylated when compared with serine phosphorylation of wild-type DMT1 (Figure 5). Subsequently, the transport of iron by cells expressing the serine mutant was tested using the ^{55}Fe tracer assay. As shown in Figure 5B,C, expression of the S^{43}A-HA mutant produced lower ^{55}Fe uptake compared with cells expressing wild-type DMT1. The input controls (Figure 5A) confirm that the expression of wild-type and the S^{43}A mutant in transfected HEK293T cells are similar, suggesting that the change in iron uptake reflects altered activity of the latter. Both the rate and extent of iron transport were reduced in cells expressing S^{43}A-HA compared with wild-type DMT1-HA.

To test the potential role of phosphorylation in DMT1 transport function, the effects of the serine/threonine protein kinase inhibitor staurosporine on iron uptake were determined. Staurosporine inhibited DMT1-mediated ^{55}Fe uptake in a dose-dependent manner (Figure 6A). To confirm the inhibition of protein

Biochemical Journal (2016) **473** 4243–4254
DOI: 10.1042/BCJ20160674

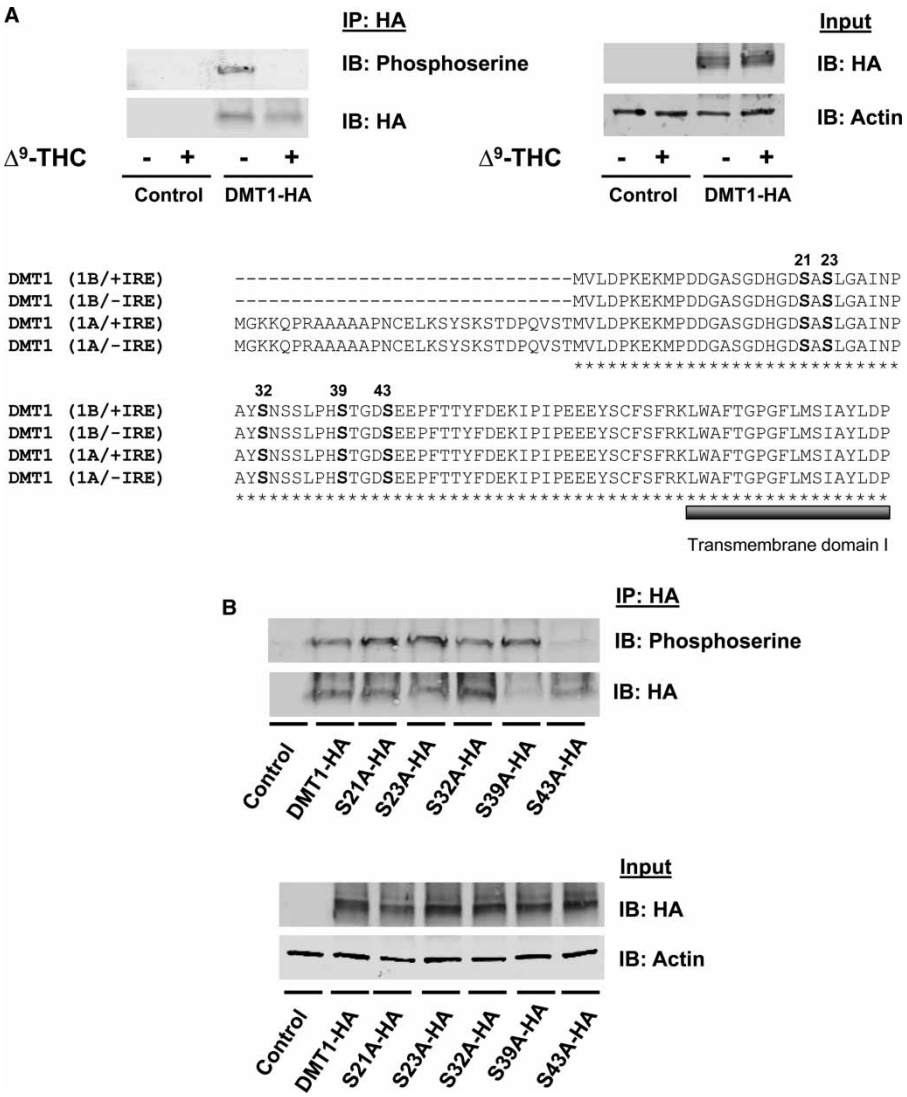

Figure 4. Serine phosphorylation of DMT1 is blocked by Δ^9-THC.

(**A**) HEK293T cells were transiently transfected with an empty vector or DMT1-HA. Cells were preincubated with a phosphatase inhibitor in PBS++ at 37°C for 15 min and then spun down, resuspended in uptake buffer containing a phosphatase inhibitor with 50 μM Δ^9-THC or control vehicle (0.5% DMSO, v/v) at 37°C for 20 min. After immunoprecipitation with anti-HA, samples were immunoblotted to determine serine phosphorylation (*IP: HA* and *IB: Phosphoserine*) compared with immunoprecipitated DMT1-HA protein (*IP: HA* and *IB: HA*). Total cell lysates from the same samples (*Input*) were used to detect DMT1-HA protein (*IB: HA*) and actin was used as a loading control (*IB: Actin*). Amino acid alignment between mouse DMT1 isoforms (1B/+IRE, 1B/−IRE, 1A/+IRE and 1A/−IRE) was generated with ClustalW. The predicted phosphorylation sites are located in a conserved region (marked with bold letters) before the first predicted transmembrane domain (marked with a bold, gray line under amino acid sequence). (**B**) HEK293 cells were transfected to express DMT1-HA and serine mutants (S^{21}A-HA, S^{23}A-HA, S^{32}A-HA, S^{39}A-HA and S^{43}A-HA). DMT1 was immunoprecipitated from the cell lysates with anti-HA antibody (*IP: HA*) and immunoblotted with antiphosphoserine antibody (*IP: HA* and *IB: Phosphoserine*). Blots were then stripped and reprobed with anti-HA (*IP: HA* and *IB: HA*) as a loading control. Total cell lysates from the same samples (*Input*) were used to detect total abundance of DMT1-HA protein and actin.

kinase activity not only blocked Fe transport but was also associated with reduced serine phosphorylation, HEK293T cells transiently transfected to express HA-tagged DMT1 were treated with or without staurosporine, and anti-HA antibodies were used to immunoprecipitate HA-DMT1 from cell lysates to detect phosphoserine. As predicted, serine phosphorylation of HA-DMT1 was reduced in cells treated with staurosporine compared

Biochemical Journal (2016) 473 4243–4254
DOI: 10.1042/BCJ20160674

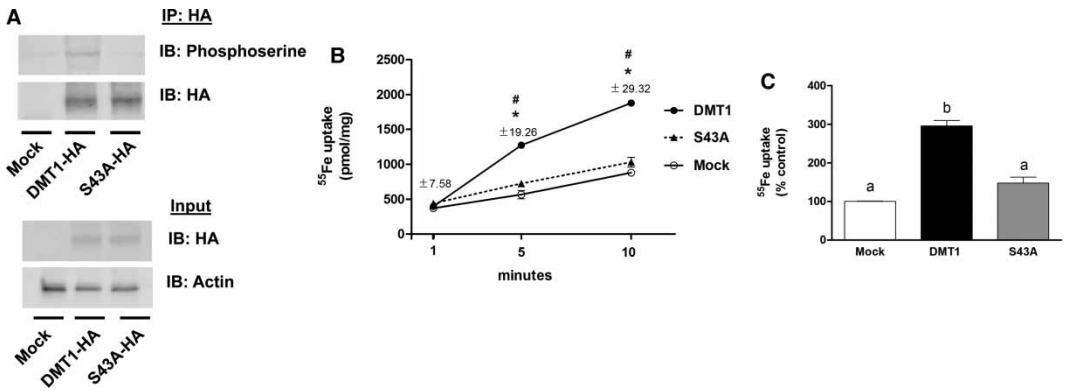

Figure 5. DMT1 phosphorylation at serine 43.

(**A**) HEK293T cells were transfected to express DMT1-HA or S43A-HA, and immunoprecipitation and immunoblot analysis were performed as described in Figure 3. (**B**) Time course of iron uptake by HEK293T cells transfected to express HA-DMT1 (closed circles) or HA-DMT1(S43A) (closed triangles) compared with mock-transfected control (empty circles) cells ($n = 3$). Similar results were obtained in at least two independent experiments. $^{*}P < 0.05$ vs. control; $^{\#}P < 0.05$ vs. S43A. SEM values are provided since errors bars are too small to visualize. (**C**) The extent of iron uptake over a 20-min incubation period was determined for HEK293T cells transfected to express DMT1-HA (filled bar), S43A-HA (gray bar) or mock-transfected (open bar). Results shown are means ± SEM ($n = 3$) with similar results obtained in at least two independent experiments ($n = 3$). Means with different letters are significantly different by one-way ANOVA followed by Tukey's multiple comparisons test ($P < 0.0001$).

with vehicle-treated control cells (Figure 6B). Figure 6C shows densitometric data obtained from two independent experiments with a 50% decrease in HA-DMT1 phosphorylation in staurosporine-treated cells. It has been shown that staurosporine induces apoptotic cell death in many different cell lines [30–32]. However, in our experiments, we did not observe any signs of cell death over the short 20 min time course of incubation (Y.A. S., personal observation).

Discussion

Previous studies from our research group applied chemical genetics to advance our understanding of different pathways of iron uptake through the discovery of transport inhibitors [13,33–35]. The bioactive small molecule Δ^9-THC was identified to block iron uptake by DMT1 in HEK293T(DMT1) cells [13]. The present study shows that the CB2 receptor is responsible for mediating the effects of Δ^9-THC on DMT1 activity in this cell line. In Δ^9-THC-treated cells, serine phosphorylation of DMT1 was significantly reduced. These observations indicate that the transporter's function can be regulated by limiting its phosphorylation or promoting its dephosphorylation. Consistent with this model, site-directed mutagenesis studies revealed that conversion of DMT1 Ser43 to Ala results in loss of phosphorylation and iron uptake activity. All of these functional effects correlate with inhibition of uptake observed in the presence of cannabinoid agonists.

The fact that Ser43 is present in all DMT1 isoforms suggests that regulation at this site is independent of the C-terminus of the protein; i.e. occurring in both +IRE and −IRE isoforms. Previous studies reported that Nramp1 (natural resistance-associated macrophage protein) [36], a macrophage-specific homolog of Nramp2 or DMT1 [37], is also post-translationally modified by phosphorylation [38]. Although specific phosphorylation site(s) have not been determined, the Nramp1 protein contains several possible PKC and casein kinase II (CK-2) sites [38,39]. Barton et al. [39] have shown that a peptide corresponding to the N-terminal domain of Nramp1 is phosphorylated and suggested that this modification reflects PKC activity. Beyond the preliminary identification of Nramp1 as a phosphoprotein, little is known about functional effects of this modification. Our observation is the first report of DMT1 (Nramp2) phosphorylation. Computer-based programs, such as KinasePhos [40], GPS (group-based prediction system) [41] and PPSP (prediction of PK-specific phosphorylation site) [42], all indicate that the Ser43 in DMT1 is a potential site for protein kinase A/G/C family members as well as CK-2. Further research is necessary to precisely define the kinase(s) involved in recognition of the Nramp transporter family and how this post-translational modification affects their transport mechanism. It has been suggested that PKCβ could play a role in Nramp1 regulation, based on regulation of this

Biochemical Journal (2016) **473** 4243–4254
DOI: 10.1042/BCJ20160674

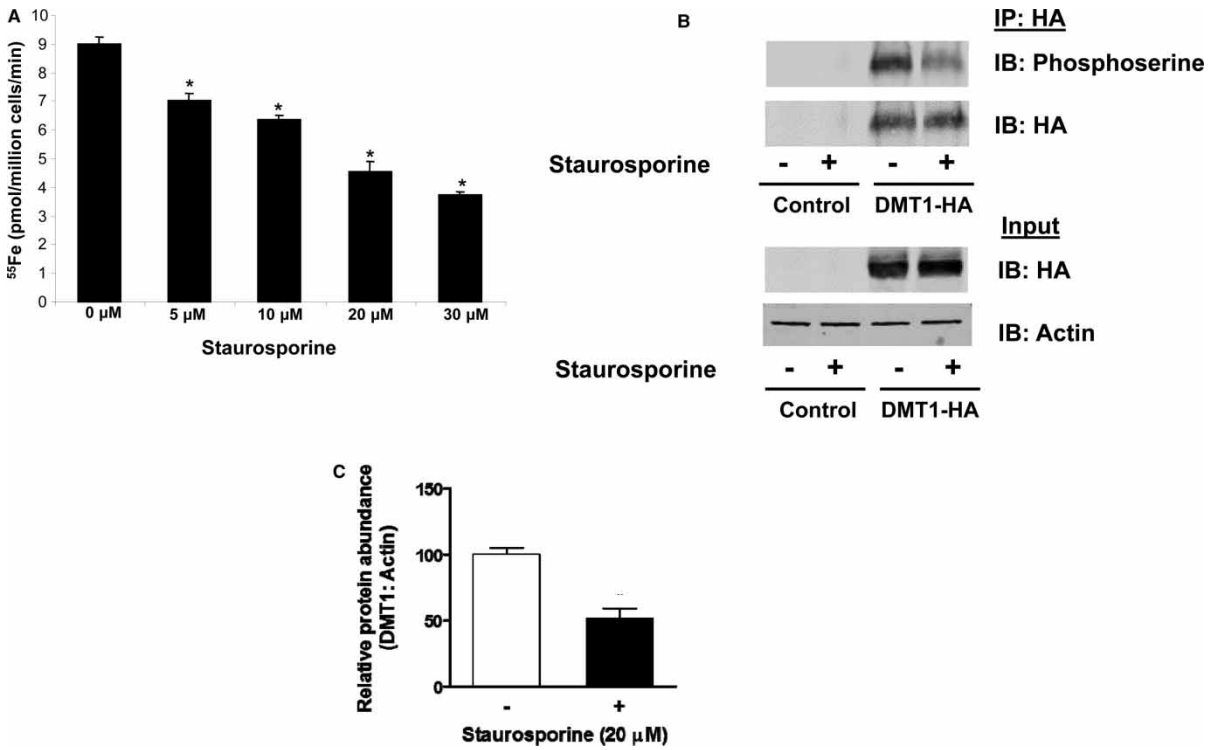

Figure 6. Staurosporine inhibits DMT1 transport and reduces serine phosphorylation.

(**A**) Iron uptake by HEK293T(DMT1) cells was assayed after incubation with indicated concentrations of staurosporine in phosphate-buffered saline with glucose (PBSG)++ at 37°C for 20 min. The histogram represents three experiments done in triplicate and results shown are mean values ± SEM for inhibition, $^{*}P < 0.001$. (**B**) Serine phosphorylation of DMT1 was determined by immunoprecipitation as described in Figure 3, except after a preincubation step with a phosphatase inhibitor in PBS++ at 37°C for 15 min, followed by assays containing a phosphatase inhibitor with 20 µM staurosporine or vehicle (0.5% DMSO, v/v) at 37°C for 20 min. Immunoprecipitation was performed using an anti-HA antibody (*IP: HA*) and immunoblotting was performed (*IP: HA* and *IB: Phosphoserine*) in comparison with immunoprecipitated DMT1-HA protein (*IP: HA* and *IB: HA*). Total cell lysates from the same samples (*Input*) were used to detect DMT1-HA protein (*IB: HA*) and actin was used as a loading control (*IB: Actin*). (**C**) Mean ratio of DMT1-HA: Actin ± SD from untreated cells (–) and cells treated with staurosporine (+) determined by densitometry of two independent experiments as described in **B**.

kinase by iron [43]. We have found that staurosporine, a broad spectrum inhibitor of both protein kinases PKA and PKC [44], reduces both DMT1 transport activity and phosphorylation, but further study is necessary to identify the DMT1 serine kinase and its relationship to other Nramp family kinases.

Although the C-termini of DMT1 isoforms have been shown to direct subcellular trafficking [27], the possibility that phosphorylation of the N-terminal Ser43 redirects subcellular localization of DMT1 to modulate its function must be considered [45]. It is interesting to note that the peripheral benzodiazepine receptor-associated protein 7 (PAP7) has been implicated in DMT1 trafficking [46]. This factor is functionally linked with the G-protein-coupled benzodiazepine receptor and associates with a cAMP-dependent kinase [47]. In a similar fashion, CB2 might regulate phosphorylation or dephosphorylation of DMT1 through a third partner akin to PAP7. We have attempted to study changes in DMT1 cellular localization upon cannabinoid treatment, as well as in response to kinase inhibitors, but failed to observe major redistribution of transporters in HEK293T(DMT1) cells or in HEK cells transiently overexpressing the HA-tagged DMT1. Both fluorescence confocal microscopy and cell surface biotinylation did detect surface transporters (data not shown) as previously demonstrated [17]. Further work is necessary to determine how phosphorylation of DMT1's N-terminus may affect iron transport. It has been shown that the copper transporter ATP7B is basally phosphorylated and becomes hyperphosphorylated in response to increased copper levels and although the functional consequences have yet to be fully determined, this activity does not affect membrane trafficking [48].

Biochemical Journal (2016) **473** 4243–4254
DOI: 10.1042/BCJ20160674

To our knowledge, the demonstration that CB2 modulates iron uptake activity is also the first report of endocrine receptor regulation of DMT1 transport. A growing body of evidence has shown the expression of CB2 receptors in microglial cells, astrocytes and some neuron populations [49]. The function of CB2 in microglia, the macrophages of the brain, is of particular interest since receptor activation decreases the *in vitro* production of proinflammatory molecules in rat [50,51] and human [52] microglial cells. CB2 activation also reduces the release of proinflammatory factors in a model of hypoxic–ischemic brain damage in newborn rats [53] and in Huntington's disease [54]. Moreover, recent evidence shows that microglia express a functional endocannabinoid signaling system and that CB2 receptors control their immune-related functions [55]. Iron is also an important regulator of immune cell function [56], and CB2 regulation of DMT1 iron uptake activity could potentially reflect an important physiological response associated with iron withdrawal during anti-inflammatory responses [57]. Our work in an immortalized microglial cell line has recently demonstrated that the CB2 selective agonist JWH-015 markedly reduces inflammation promoted by the Alzheimer's disease protein amyloid-β [58]. A decrease in iron import would be consistent with this effect. While there are many studies on iron regulation and its effects on peripheral macrophages and immune function, very little is known regarding microglial iron handling [59]. Thus, it will be interesting to test whether microglia utilize the cannabinoid signaling system to modulate cellular iron status through the regulation of DMT1 function.

Further studies are also warranted to determine the detailed mechanism through which DMT1 phosphorylation is responsible for controlling its activity. DMT1 is regulated at transcriptional [6,60], post-transcriptional [8,9] and post-translational levels [61]. Our study demonstrates that phosphorylation at S^{43} is linked to a functionally active state of the transporter's function. Understanding how DMT1 function is modified by this post-translational modification may provide insights about the membrane transport of iron. Moreover, since Ser43 phosphorylation activates DMT1 under basal conditions, dephosphorylation at this site provides an interesting potential target for pharmacological tools to treat diseases of iron overload.

Abbreviations

CB1, cannabinoid receptor type 1; CB2, cannabinoid receptor type 2; CK-2, casein kinase II; DMT1, divalent metal transporter-1; G-protein, GTP-binding protein; HA, hemagglutinin; IRE, iron responsive element; MAPK/ERK, mitogen-activated protein kinases/extracellular signal-regulated kinases; PAP7, peripheral benzodiazepine receptor-associated protein 7; PKA, cAMP-protein kinase; PKC, protein kinase C; THC, tetrahydrocannabinol.

Author Contribution

Y.A.S., R.K. and H.W. conducted experiments. All authors contributed to conceptual design of experiments. Y.A.S. and R.K. wrote sections of this manuscript and M.W.R. is responsible for final editing.

Funding

Research reported in this publication was supported by grants from the National Institutes of Health under the awards R01 DK064750 and R21 DA0255. Y.A.S. was supported by a grant from the National Institutes of Health under award number [K99 ES024340].

Acknowledgements

We appreciate the technical help from Jose Carlo Sosa in conducting the MAPK/ERK inhibition study, and appreciate advice from Dr Jonghan Kim, Northeastern University, on Sigmaplot analyses.

Competing Interests

The Authors declare that there are no competing interests associated with the manuscript.

References

1 Gunshin, H., Fujiwara, Y., Custodio, A.O., Direnzo, C., Robine, S. and Andrews, N.C. (2005) Slc11a2 is required for intestinal iron absorption and erythropoiesis but dispensable in placenta and liver. *J. Clin. Invest.* **115**, 1258–1266 doi:10.1172/JCI24356

2 Fleming, M.D., Romano, M.A., Su, M.A., Garrick, L.M., Garrick, M.D. and Andrews, N.C. (1998) Nramp2 is mutated in the anemic Belgrade (b) rat: evidence of a role for Nramp2 in endosomal iron transport. *Proc. Natl Acad. Sci. USA* **95**, 1148–1153 doi:10.1073/pnas.95.3.1148

3 Shawki, A., Knight, P.B., Maliken, B.D., Niespodzany, E.J. and Mackenzie, B. (2012) Chapter five — H^+-coupled divalent metal-ion transporter-1: functional properties, physiological roles and therapeutics. *Curr. Top. Membr.* **70**, 169–214 doi:10.1016/B978-0-12-394316-3.00005-3

4 Gunshin, H., Mackenzie, B., Berger, U.V., Gunshin, Y., Romero, M.F., Boron, W.F. et al. (1997) Cloning and characterization of a mammalian proton-coupled metal-ion transporter. *Nature* **388**, 482–488 doi:10.1038/41343

5 Hubert, N. and Hentze, M.W. (2002) Previously uncharacterized isoforms of divalent metal transporter (DMT)-1: implications for regulation and cellular function. *Proc. Natl Acad. Sci. USA* **99**, 12345–12350 doi:10.1073/pnas.192423399
6 Mastrogiannaki, M., Matak, P., Keith, B., Simon, M.C., Vaulont, S. and Peyssonnaux, C. (2009) HIF-2α, but not HIF-1α, promotes iron absorption in mice. *J. Clin. Invest.* **119**, 1159–1166 doi:10.1172/JCI38499
7 Shah, Y.M., Matsubara, T., Ito, S., Yim, S.-H. and Gonzalez, F.J. (2009) Intestinal hypoxia-inducible transcription factors are essential for iron absorption following iron deficiency. *Cell Metab.* **9**, 152–164 doi:10.1016/j.cmet.2008.12.012
8 Gunshin, H., Allerson, C.R., Polycarpou-Schwarz, M., Rofts, A., Rogers, J.T., Kishi, F. et al. (2001) Iron-dependent regulation of the divalent metal ion transporter. *FEBS Lett.* **509**, 309–316 doi:10.1016/S0014-5793(01)03189-1
9 Galy, B., Ferring-Appel, D., Becker, C., Gretz, N., Gröne, H.-J., Schümann, K. et al. (2013) Iron regulatory proteins control a mucosal block to intestinal iron absorption. *Cell Rep.* **3**, 844–857 doi:10.1016/j.celrep.2013.02.026
10 Canonne-Hergaux, F., Gruenheid, S., Ponka, P. and Gros, P. (1999) Cellular and subcellular localization of the Nramp2 iron transporter in the intestinal brush border and regulation by dietary iron. *Blood* **93**, 4406–4417 PMID:10361139
11 Canonne-Hergaux, F., Zhang, A.-S., Ponka, P. and Gros, P. (2001) Characterization of the iron transporter DMT1 (NRAMP2/DCT1) in red blood cells of normal and anemic *mk/mk* mice. *Blood* **98**, 3823–3830 doi:10.1182/blood.V98.13.3823
12 Foot, N.J., Dalton, H.E., Shearwin-Whyatt, L.M., Dorstyn, L., Tan, S.-S., Yang, B. et al. (2008) Regulation of the divalent metal ion transporter DMT1 and iron homeostasis by a ubiquitin-dependent mechanism involving Ndfips and WWP2. *Blood* **112**, 4268–4275 doi:10.1182/blood-2008-04-150953
13 Wetli, H.A., Buckett, P.D. and Wessling-Resnick, M. (2006) Small-molecule screening identifies the selanazal drug ebselen as a potent inhibitor of DMT1-mediated iron uptake. *Chem. Biol.* **13**, 965–972 doi:10.1016/j.chembiol.2006.08.005
14 Howlett, A.C. (2002) The cannabinoid receptors. *Prostaglandins Other Lipid Mediat.* **68–69**, 619–631 doi:10.1016/S0090-6980(02)00060-6
15 Pacher, P., Batkai, S. and Kunos, G. (2006) The endocannabinoid system as an emerging target of pharmacotherapy. *Pharmacol. Rev.* **58**, 389–462 doi:10.1124/pr.58.3.2
16 Caulfield, M.P. and Brown, D.A. (1992) Cannabinoid receptor agonists inhibit Ca current in NG108-15 neuroblastoma cells via a pertussis toxin-sensitive mechanism. *Br. J. Pharmacol.* **106**, 231–232 doi:10.1111/j.1476-5381.1992.tb14321.x
17 Mackie, K. and Hille, B. (1992) Cannabinoids inhibit N-type calcium channels in neuroblastoma-glioma cells. *Proc. Natl Acad. Sci. USA* **89**, 3825–3829 doi:10.1073/pnas.89.9.3825
18 Pan, X., Ikeda, S.R. and Lewis, D.L. (1996) Rat brain cannabinoid receptor modulates N-type Ca^{2+} channels in a neuronal expression system. *Mol. Pharmacol.* **49**, 707–714 PMID:8609900
19 Childers, S.R., Pacheco, M.A., Bennett, B.A., Edwards, T.A., Hampson, R.E., Mu, J. et al. (1993) Cannabinoid receptors: G-protein-mediated signal transduction mechanisms. *Biochem. Soc. Symp.* **59**, 27–50 PMID:8192687
20 Mackie, K., Lai, Y., Westenbroek, R. and Mitchell, R. (1995) Cannabinoids activate an inwardly rectifying potassium conductance and inhibit Q-type calcium currents in AtT20 cells transfected with rat brain cannabinoid receptor. *J. Neurosci.* **15**, 6552–6561 PMID:7472417
21 Liu, Y.-Q., Qiu, F., Qiu, C.-Y., Cai, Q., Zou, P., Wu, H. et al. (2012) Cannabinoids inhibit acid-sensing ion channel currents in rat dorsal root ganglion neurons. *PLoS ONE* **7**, e45531 doi:10.1371/journal.pone.0045531
22 Shivachar, A.C. (2007) Cannabinoids inhibit sodium-dependent, high-affinity excitatory amino acid transport in cultured rat cortical astrocytes. *Biochem. Pharmacol.* **73**, 2004–2011 doi:10.1016/j.bcp.2007.03.018
23 Touret, N., Furuya, W., Forbes, J., Gros, P. and Grinstein, S. (2003) Dynamic traffic through the recycling compartment couples the metal transporter Nramp2 (DMT1) with the transferrin receptor. *J. Biol. Chem.* **278**, 25548–25557 doi:10.1074/jbc.M212374200
24 Picard, V., Govoni, G., Jabado, N. and Gros, P. (2000) Nramp 2 (DCT1/DMT1) expressed at the plasma membrane transports iron and other divalent cations into a calcein-accessible cytoplasmic pool. *J. Biol. Chem.* **275**, 35738–35745 doi:10.1074/jbc.M005387200
25 Czachorowski, M., Lam-Yuk-Tseung, S., Cellier, M. and Gros, P. (2009) Transmembrane topology of the mammalian Slc11a2 iron transporter. *Biochemistry* **48**, 8422–8434 doi:10.1021/bi900606y
26 Lam-Yuk-Tseung, S., Touret, N., Grinstein, S. and Gros, P. (2005) Carboxyl-terminus determinants of the iron transporter DMT1/SLC11A2 isoform II (–IRE/1B) mediate internalization from the plasma membrane into recycling endosomes. *Biochemistry* **44**, 12149–12159 doi:10.1021/bi050911r
27 Lam-Yuk-Tseung, S. and Gros, P. (2006) Distinct targeting and recycling properties of two isoforms of the iron transporter DMT1 (NRAMP2, Slc11A2). *Biochemistry* **45**, 2294–2301 doi:10.1021/bi052307m
28 Hornbeck, P.V., Kornhauser, J.M., Tkachev, S., Zhang, B., Skrzypek, E., Murray, B. et al. (2012) Phosphositeplus: a comprehensive resource for investigating the structure and function of experimentally determined post-translational modifications in man and mouse. *Nucleic Acids Res.* **40**, D261–D270 doi:10.1093/nar/gkr1122
29 Blom, N., Gammeltoft, S. and Brunak, S. (1999) Sequence and structure-based prediction of eukaryotic protein phosphorylation sites. *J. Mol. Biol.* **294**, 1351–1362 doi:10.1006/jmbi.1999.3310
30 Wolf, C.M. and Eastman, A. (1999) The temporal relationship between protein phosphatase, mitochondrial cytochrome *c* release, and caspase activation in apoptosis. *Exp. Cell Res.* **247**, 505–513 doi:10.1006/excr.1998.4380
31 Belmokhtar, C.A., Hillion, J. and Segal-Bendirdjian, E. (2001) Staurosporine induces apoptosis through both caspase-dependent and caspase-independent mechanisms. *Oncogene* **20**, 3354–3362 doi:10.1038/sj.onc.1204436
32 Yuste, V.J., Sanchez-Lopez, I., Sole, C., Encinas, M., Bayascas, J.R., Boix, J. et al. (2002) The prevention of the staurosporine-induced apoptosis by Bcl-X_L, but not by Bcl-2 or caspase inhibitors, allows the extensive differentiation of human neuroblastoma cells. *J. Neurochem.* **80**, 126–139 doi:10.1046/j.0022-3042.2001.00695.x
33 Buckett, P.D. and Wessling-Resnick, M. (2009) Small molecule inhibitors of divalent metal transporter-1. *Am. J. Physiol. Gastrointest. Liver Physiol.* **296**, G798–G804 doi:10.1152/ajpgi.90342.2008
34 Horonchik, L. and Wessling-Resnick, M. (2008) The small-molecule iron transport inhibitor ferristatin/NSC306711 promotes degradation of the transferrin receptor. *Chem. Biol.* **15**, 647–653 doi:10.1016/j.chembiol.2008.05.011
35 Brown, J.X., Buckett, P.D. and Wessling-Resnick, M. (2004) Identification of small molecule inhibitors that distinguish between non-transferrin bound iron uptake and transferrin-mediated iron transport. *Chem. Biol.* **11**, 407–416 doi:10.1016/j.chembiol.2004.02.016

Biochemical Journal (2016) **473** 4243–4254
DOI: 10.1042/BCJ20160674

36 Vidal, S.M., Malo, D., Vogan, K., Skamene, E. and Gros, P. (1993) Natural resistance to infection with intracellular parasites: isolation of a candidate for *Bcg*. *Cell* **73**, 469–485 doi:10.1016/0092-8674(93)90135-D

37 Malo, D. and Skamene, E. (1994) Genetic control of host resistance to infection. *Trends Genet.* **10**, 365–371 doi:10.1016/0168-9525(94)90133-3

38 Vidal, S.M., Pinner, E., Lepage, P., Gauthier, S. and Gros, P. (1996) Natural resistance to intracellular infections: Nramp1 encodes a membrane phosphoglycoprotein absent in macrophages from susceptible (Nramp1 D169) mouse strains. *J. Immunol.* **157**, 3559–3568 PMID:8871656

39 Barton, C.H., White, J.K., Roach, T.I. and Blackwell, J.M. (1994) NH2-terminal sequence of macrophage-expressed natural resistance-associated macrophage protein (Nramp) encodes a proline/serine-rich putative Src homology 3-binding domain. *J. Exp. Med.* **179**, 1683–1687 doi:10.1084/jem.179.5.1683

40 Huang, H.-D., Lee, T.-Y., Tzeng, S.-W. and Horng, J.-T. (2005) Kinasephos: a web tool for identifying protein kinase-specific phosphorylation sites. *Nucleic Acids Res.* **33**, W226–W229 doi:10.1093/nar/gki471

41 Xue, Y., Zhou, F., Zhu, M., Ahmed, K., Chen, G. and Yao, X. (2005) GPS: a comprehensive www server for phosphorylation sites prediction. *Nucleic Acids Res.* **33**, W184–W187 doi:10.1093/nar/gki393

42 Xue, Y., Li, A., Wang, L., Feng, H. and Yao, X. (2006) PPSP: prediction of PK-specific phosphorylation site with Bayesian decision theory. *BMC Bioinformatics* **7**, 163 doi:10.1186/1471-2105-7-163

43 Alcantara, O., Obeid, L., Hannun, Y., Ponka, P. and Boldt, D.H. (1994) Regulation of protein kinase C (PKC) expression by iron: effect of different iron compounds on PKC-beta and PKC-alpha gene expression and role of the 5′-flanking region of the PKC-beta gene in the response to ferric transferrin. *Blood* **84**, 3510–3517 PMID:7949105

44 Rüegg, U.T. and Gillian, B. (1989) Staurosporine, K-252 and UCN-01: potent but nonspecific inhibitors of protein kinases. *Trends Pharmacol. Sci.* **10**, 218–220 doi:10.1016/0165-6147(89)90263-0

45 Ma, Y., Yeh, M., Yeh, K.-y. and Glass, J. (2006) Iron imports. V. Transport of iron through the intestinal epithelium. *Am. J. Physiol. Gastrointest. Liver Physiol.* **290**, G417–G422 doi:10.1152/ajpgi.00489.2005

46 Okazaki, Y., Ma, Y., Yeh, M., Yin, H., Li, Z., Yeh, K.-y. et al. (2012) DMT1 (IRE) expression in intestinal and erythroid cells is regulated by peripheral benzodiazepine receptor-associated protein 7. *Am. J. Physiol. Gastrointest. Liver Physiol.* **302**, G1180–G1190 doi:10.1152/ajpgi.00545.2010

47 Li, H., Degenhardt, B., Tobin, D., Yao, Z.-x., Tasken, K. and Papadopoulos, V. (2001) Identification, localization, and function in steroidogenesis of PAP7: a peripheral-type benzodiazepine receptor- and PKA (RIα)-associated protein. *Mol. Endocrinol.* **15**, 2211–2228 doi:10.1210/mend.15.12.0736

48 Braiterman, L.T., Gupta, A., Chaerkady, R., Cole, R.N. and Hubbard, A.L. (2015) Communication between the N and C termini is required for copper-stimulated Ser/Thr phosphorylation of Cu(I)-ATPase (ATP7B). *J. Biol. Chem.* **290**, 8803–8819 doi:10.1074/jbc.M114.627414

49 Fernández-Ruiz, J., Romero, J., Velasco, G., Tolón, R.M., Ramos, J.A. and Guzman, M. (2007) Cannabinoid CB2 receptor: a new target for controlling neural cell survival? *Trends Pharmacol. Sci.* **28**, 39–45 doi:10.1016/j.tips.2006.11.001

50 Facchinetti, F., Del Giudice, E., Furegato, S., Passarotto, M. and Leon, A. (2003) Cannabinoids ablate release of TNFα in rat microglial cells stimulated with lypopolysaccharide. *Glia* **41**, 161–168 doi:10.1002/glia.10177

51 Puffenbarger, R.A., Boothe, A.C. and Cabral, G.A. (2000) Cannabinoids inhibit LPS-inducible cytokine mRNA expression in rat microglial cells. *Glia* **29**, 58–69 doi:10.1002/(SICI)1098-1136(20000101)29:1<58::AID-GLIA6>3.0.CO;2-W

52 Stella, N. (2004) Cannabinoid signaling in glial cells. *Glia* **48**, 267–277 doi:10.1002/glia.20084

53 Fernández-López, D., Martínez-Orgado, J., Nuñez, E., Romero, J., Lorenzo, P., Moro, M.Á. et al. (2006) Characterization of the neuroprotective effect of the cannabinoid agonist WIN-55212 in an in vitro model of hypoxic-ischemic brain damage in newborn rats. *Pediatr. Res.* **60**, 169–173 doi:10.1203/01.pdr.0000228839.00122.6c

54 Fernández-Ruiz, J. and González, S. (2005) Cannabinoid control of motor function at the basal ganglia. *Handb. Exp. Pharmacol.* **168**, 479–507 doi:10.1007/3-540-26573-2_16

55 Stella, N. (2009) Endocannabinoid signaling in microglial cells. *Neuropharmacology* **56**(Suppl 1), 244–253 doi:10.1016/j.neuropharm.2008.07.037

56 Theurl, I., Fritsche, G., Ludwiczek, S., Garimorth, K., Bellmann-Weiler, R. and Weiss, G. (2005) The macrophage: a cellular factory at the interphase between iron and immunity for the control of infections. *Biometals* **18**, 359–367 doi:10.1007/s10534-005-3710-1

57 Kim, J., Molina, R.M., Donaghey, T.C., Buckett, P.D., Brain, J.D. and Wessling-Resnick, M. (2011) Influence of DMT1 and iron status on inflammatory responses in the lung. *Am. J. Physiol. Lung Cell. Mol. Physiol.* **300**, L659–L665 doi:10.1152/ajplung.00343.2010

58 McCarthy, R.C., Lu, D.-Y., Alkhateeb, A., Gardeck, A.M., Lee, C.-H. and Wessling-Resnick, M. (2016) Characterization of a novel adult murine immortalized microglial cell line and its activation by amyloid-beta. *J. Neuroinflammation* **13**, 21 doi:10.1186/s12974-016-0484-z

59 Zhang, X., Surguladze, N., Slagle-Webb, B., Cozzi, A. and Connor, J.R. (2006) Cellular iron status influences the functional relationship between microglia and oligodendrocytes. *Glia* **54**, 795–804 doi:10.1002/glia.20416

60 Shah, S.V. and Rajapurkar, M.M. (2009) The role of labile iron in kidney disease and treatment with chelation. *Hemoglobin* **33**, 378–385 doi:10.3109/03630260903212233

61 Foot, N.J., Leong, Y.A., Dorstyn, L.E., Dalton, H.E., Ho, K., Zhao, L. et al. (2011) Ndfip1-deficient mice have impaired DMT1 regulation and iron homeostasis. *Blood* **117**, 638–646 doi:10.1182/blood-2010-07-295287

